Title

Successful treatment of murine autoimmune cholangitis by parabiosis: Implications for hematopoietic therapy

Authors

Yang, Jing-Bo
Wang, Yin-Hu
Yang, Wei
et al.

Publication Date

2016

DOI

10.1016/j.jaut.2015.09.002

Peer reviewed

HHS Public Access

Author manuscript

J Autoimmun. Author manuscript; available in PMC 2016 April 12.

Published in final edited form as:

J Autoimmun. 2016 January ; 66: 108–117. doi:10.1016/j.jaut.2015.09.002.

Successful Treatment of Murine Autoimmune Cholangitis by Parabiosis: Implications for Hematopoietic Therapy

Jing-Bo Yang[1,*], **Yin-Hu Wang**[1,*], **Wei Yang**[1], **Fang-Ting Lu**[1], **Hong-Di Ma**[1], **Zhi-Bin Zhao**[1], **Yan-Jie Jia**[1], **Wei Tang**[1], **Koichi Tsuneyama**[2], **William M. Ridgway**[3], **M. Eric Gershwin**[4], and **Zhe-Xiong Lian**[1,5]

Jing-Bo Yang: yjingb@mail.ustc.edu.cn; Yin-Hu Wang: wangyh8@mail.ustc.edu.cn; Wei Yang: ywei0702@mail.ustc.edu.cn; Fang-Ting Lu: fangting@mail.ustc.edu.cn; Hong-Di Ma: mahongdi@ustc.edu.cn; Zhi-Bin Zhao: zzbin@mail.ustc.edu.cn; Yan-Jie Jia: jyanjie@mail.ustc.edu.cn; Wei Tang: wayne012@mail.ustc.edu.cn; Koichi Tsuneyama: tsuneyama.koichi@tokushima-u.ac.jp; William M. Ridgway: ridgwawm@uc.edu; M. Eric Gershwin: megershwin@ucdavis.edu; Zhe-Xiong Lian: zxlian1@ustc.edu.cn

[1]Liver Immunology Laboratory, Institute of Immunology and The CAS Key Laboratory of Innate Immunity and Chronic Disease, School of Life Sciences and Medical Center, University of Science and Technology of China, Hefei, Anhui 230027

[2]Department of Diagnostic Pathology, Graduate School of Medicine and Pharmaceutical Science for Research, University of Toyama, Toyama 930-0194, Japan

[3]Division of Immunology, Allergy and Rheumatology, University of Cincinnati, Cincinnati, OH 45220

[4]Division of Rheumatology, Allergy and Clinical Immunology, University of California at Davis School of Medicine, Davis, CA 95616, USA

[5]Innovation Center for Cell Signaling Network, Hefei National Laboratory for Physical Sciences at Microscale, Hefei, Anhui 230027, China

Abstract

There is a significant unmet need in the treatment of primary biliary cirrhosis (PBC) despite significant data on the effector pathways that lead to biliary duct damage. We focused attention on a murine model of PBC, the dominant negative transforming growth factor β receptor II (Tg) mice. To further define the pathways that lead to biliary pathology in these mice, we developed Tg mice deleted of CD4 cells ($CD4^{-/-}$Tg).

Interestingly, these mice developed more severe cholangitis than control Tg mice. These mice, which lack CD4 cells, manifested increased levels of IFN-γ produced by effector CD8 cells. It appears that increased cholangitis is due to the absence of CD4 Treg cells. Based on these data, we parabiosed $CD4^{-/-}$Tg mice with established disease at 8–9 weeks of age with C57BL/6 control mice. Such parabiotic “twins” had a significant reduction in autoimmune cholangitis, even though they had established pathology at the time of surgery. We prepared mixed bone marrow chimera

Correspondence to: Zhe-Xiong Lian, M.D., Ph.D., Liver Immunology Laboratory, Institute of Immunology and School of Life Sciences, University of Science and Technology of China, Hefei 230027, China; Phone: +86-551-63600317; Fax: +86-551-63600317; zxlian1@ustc.edu.cn or M. Eric Gershwin, M.D., Division of Rheumatology, Allergy and Clinical Immunology, University of California at Davis School of Medicine, 451 Health Sciences Drive, Suite 6510, Davis, CA 95616; telephone: 530-752-2884; fax: 530-752-4669; megershwin@ucdavis.edu.

*These authors contributed equally to this work.

mice constructed from $CD4^{-/-}$Tg and $CD8^{-/-}$ mice and not only was cholangitis improved, but a decrease in terminally differentiated $CD8^+$ T effector cells in the presence of wild type CD4 cells was noted. In conclusion, “correcting” the CD4 T cell subset, even in the presence of pathogenic CD8 T cells, is effective in treating autoimmune cholangitis.

Keywords

Primary biliary cirrhosis; cholangitis; $CD4^+$ T cells; regulatory T cells; bone marrow chimeric mice; parabiosis

Introduction

Primary biliary cirrhosis is a prototypical organ specific autoimmune biliary disease characterized by portal inflammation, leucocyte-mediated intra-hepatic bile duct damage and anti-mitochondrial antibodies [1, 2]. There is extensive data on the putative effector pathways that lead to biliary destruction and the relationships between loss of tolerance and biliary pathology[3–7]. The destruction of bile ducts is associated with cholestasis, resulting in cirrhosis and liver failure. However, most patients develop clinical symptoms long after the initial loss of immune tolerance. To define the earliest immunopathological events in PBC, we have studied dominant negative transforming growth factor receptor type II transgenic mice (Tg) [8] in which dnTGFβRII is expressed on both $CD4^+$ and $CD8^+$ T cells. T lymphocyte specific impairment of TGF-β signaling results in autoimmune cholangitis mediated by $CD8^+$ T [9] and B cells [10, 11] in the presence of pro-inflammatory cytokines [11–14], and accompanied by anti-mitochondrial antibodies of the same specificity as human PBC. Moreover, transfer of Tg -derived $CD8^+$ T cells alone to lymphopenic mice generates a robust cholangitis [9]. Importantly, when the $CD8^+$ TCR repertoire is restricted to ovalbumin (OVA), the immunologic and histologic features of PBC disappear. Further, OVA restricted Tg $CD8^+$ T cells fail to transfer biliary disease [15]. Hence, antigen-specific $CD8^+$ T cells are necessary for the pathogenesis of cholangitis in this model.

$CD4^+Foxp3^+$ regulatory T cells (Tregs) play a major role in control of excessive immune responses [16] and defects in Tregs have been reported both in PBC patients and murine PBC models. First, PBC patients, and their relatives have significantly lower frequency of $CD4^+CD25^+$ Treg cells [17]. Second, the clinical features of neonatal deficiency of CD25 included an autoimmune cholangitis that remits after bone marrow transplantation [18]. Third, Scurfy mice with complete absence of $Foxp3^+$ Tregs, develop cholangitis and high titer of serum AMAs [11], and finally mice deficient in IL-2Rα (CD25) also develop PBC [19], consistent with our observations that transfer of WT derived $CD4^+Foxp3^+$ Tregs protects against biliary disease in adoptive transfer models [20, 21]. It is unknown whether Tregs can reverse established immune dysregulation. We report herein the successful modulation of cholangitis even in animals with established pathology. The implications of these data for humans with PBC are striking, since correction of the CD4 subset deficiencies can reverse the disease even in the presence of persistent CD8 T cell abnormalities.

Materials and Methods

Mice

C57BL/6 dnTGFβRII (B6.Cg-Tg (Cd4-TGFBR2) 16Flv/J), Foxp3^{GFP} mice (Foxp3^{tm2Ayr}), CD4$^{-/-}$, CD8$^{-/-}$, congenic CD45.2, CD45.1 mice were housed under specific pathogen-free conditions in the animal facility of the School of Life Sciences of the University of Science and Technology of China. To generate CD4$^{-/-}$dnTGFβRII (CD4$^{-/-}$Tg) mice, CD4$^{-/-}$ mice were bred with Tg mice. CD4 knockout was confirmed by detecting the expression of CD4 on leucocytes by flow cytometry. Foxp3^{GFP}dnTGFβRII (Foxp3^{GFP}Tg) mice were generated by breeding male Tg mice with female Foxp3^{GFP} mice. Experiments were performed following approval of the USTC Animal Care and Use Committee.

Preparation of hepatic, splenic or mesenteric mononuclear cells

To isolate hepatic mononuclear cells, livers were ground through 200G stainless steel mesh in PBS with 0.2% BSA. The liver homogenate was pelleted by centrifuging at 450g for 5 minutes. The pellets were resuspended in 40% Percoll (GE Healthcare, Little Chalfont, United Kingdom); thence 70% Percoll was added to the bottom and centrifuged at 800g for 20 minutes at room temperature. The mononuclear cells layer was collected by centrifuging at 800g for 5 minutes. Whole spleen was disrupted between 2 microscope glass slides and red cells were lysed for 10 minutes. After neutralizing the buffer with PBS, pellets were resuspended. Mesenteric lymph nodes were disrupted between two glass slides, cells were suspended in PBS with 0.2% BSA and passed through a 70 μm nylon mesh, and mononuclear cells collected by centrifugation at 800g for 5 min. The viability of cells was confirmed by trypan blue dye exclusion.

Flow Cytometry

Cell suspensions were incubated with anti-mouse CD16/32 (Biolegend, San Diego, CA) to block the Fc receptor before cell surface staining. All flow antibodies, unless otherwise noted, were purchased from Biolegend. To identify subpopulation of lymphocytes, cells were stained with Pacific Blue-CD3 (17A2), FITC-CD8β (YTS156.7.7), Alexa647-mCD1d-Tetramer (Provided by NIH Tetramer Core Facility, NO 22188, Emory University), PerCP/Cy5.5-CD62L (MEL-14), PE-Cy7-NK1.1 (PK136), V500-B220 (RA3-6B2, BD Bioscience), Alexa Fluor 647-CD44 (IM7), APC-Cy7-CD4 (GK1.5). To distinguish donor versus recipient subpopulations in chimeric recipients, cells were stained with PerCP/Cy5.5-CD45.1 (A20), APC-CD45.2 (104), Pacific Blue-TCR-β (H57-597), V500-CD8α (53-6.7, BD Bioscience), FITC-CD44 (IM7), PE-CD19 (6D5), PE-CD62L (MEL-14), PE-Cy7-NK1.1(PK136), APC-KLRG-1 (2F1/KLRG-1), APC-Cy7-CD4 (GK1.5), PE-CD25 (PC61), GITR(DTA-1). For intracellular staining, cells were resuspended in RPMI-1640 with 10% fetal bovine serum and stimulated with Cell Stimulation Cocktail (plus protein transport inhibitors) (eBioscience, San Diego, CA) at 37°, 5% CO_2 for 3 hours. Thence cells were phenotyped for CD3, CD4, CD25, CD8β, and NK1.1, fixed with Fixation Buffer (Biolegend), and permeabilized with Permeabilization Wash Buffer (Biolegend). Intracellular staining was performed with PE-IFN-γ (XMG1.2) and PE-CTLA4 (UC10-4B9). Normal IgG isotype controls (Biolegend) were used as controls. Intracellular transcriptional factor Foxp3 was stained by Alexa647-conjugated anti-Foxp3 (150D) by a

Foxp3 staining set (eBioscience). Flow data was acquired using a flow cytometer FACS Verse (BD Bioscience). Data were analyzed using Flow Jo software (Tree Star, Inc., Ashland, OR).

Parabiosis

Pairs of 8 to 9-wk-old, female- and weight- (within 2 g) matched, wild type CD45.1 mice and $CD4^{-/-}$Tg CD45.2 mice were parabiosed [22, 23] with a modified procedure. In the same manner, wild type CD45.1×CD45.2 mice and $CD4^{-/-}$ CD45.2 mice were parabiosed as control pairs, as the strategy summarized in Figure 4A. Briefly, mice were first anesthetized by intraperitoneal injection of 1% pentobarbital sodium (Merck, Darmstadt, German) at a dose of 10 μL per gram body weight. Once the mice were anesthetized, the skin was shaved on the left side of one partner and the right side of the other partner, and sterilized with a Betadine-soaked cotton ball followed by 75% alcohol wipes. A lateral incision was made through the skin from the olecranon to knee joint of each mouse, thence the subcutaneous fascia was dissected to create 0.5 cm of free skin. The olecranon and knee joints were attached using 5-0 vicryl suture and the dorsal and ventral skins were closed by continuous 5-0 suture line. After surgery, 500 μL saline was administered subcutaneously to each mouse to prevent dehydration, and the pairs were kept on a heated pad until recovery. To prevent bacterial infections, mice were treated with Sulfamethoxazole (2 mg/mL)/Trimethoprim (0.4 mg/mL) oral suspension in water bottle for 1 week. Mice were sacrificed 4 weeks after surgery.

Generation of Bone Marrow Chimeric Mice

Recipient mice (B6 CD45.1×CD45.2 F1) were fed sterile mouse chow and water containing 1 g/L ampicillin, 1 g/L metronidazole and 1 g/L neomycin beginning one week before irradiation with 1100 rad γ-ray. $CD8^{-/-}$ CD45.1 and $CD4^{-/-}$Tg CD45.2 donor mice were used as bone marrow donors, as the strategy summarized in Figure 6A. Lineage positive cells were depleted from bone marrow cell using a series of purified antibodies including α-CD3 (17A2, Biolegend), α-B220 (RA3-6B2, Biolegend), α-CD11b (M1/70, eBioscience), α-Gr-1 (RB6-8C5, eBioscience), α-TER119 (TER-119, eBioscience) and Sheep-α-Rat IgG Dynabeads. Bone marrow lineage negative cells were mixed at a 1:1 ratio (3×10^5: 3×10^5) then transferred into recipients by intravenous injection within 24 hours after irradiation. Control recipients were transferred with 3×10^5 purified $lineage^-$ bone marrow cells derived from $CD4^{-/-}$Tg CD45.2 mice. Recipient mice were sacrificed 2 months after bone marrow transplantation.

Cell Sorting and Regulatory T cell Suppression Assay

$CD4^+$ T cells from $Foxp3^{GFP}$ and $Foxp3^{GFP}$Tg mice were first enriched by anti-CD4 magnetic microbeads (Miltenyi Biotech, Germany), thence $CD4^+$T cells were labeled with PerCP/Cy5.5-conjugated anti-CD4 antibody, and conventional $CD4^+$T cells were sorted as $CD4^+$Foxp3-GFP^-, while Tregs were sorted as $CD4^+$Foxp3-GFP^+ using a FACS Aria I (Becton Dickinson, USA). The purity was confirmed to be greater than 95%. $CD8^+$ T cells were purified from the splenocytes of $Foxp3^{GFP}$ and $Foxp3^{GFP}$Tg mice, by anti-CD8 magnetic microbeads (Miltenyi Biotech, Germany) with purity greater than 90%. Mitomycin-treated splenic cells were prepared as a source of antigen presenting cells

(APCs) by labeling cells from Foxp3^{GFP}Tg mice with PE/Cy7-conjugated NK1.1 and PE-conjugated CD4 and CD8, then sorted as NK1.1^{-}CD4^{-}CD8^{-} cells followed by treatment with 25 μg/ml Mitomycin C (Sigma, MO, USA) for 30 min at 37°C, and finally washed five times with RPMI 1640 medium (Life Technologies, OR, USA) [24]. Purified splenic conventional CD4^{+} T cells and CD8^{+} T cells from Foxp3^{GFP}Tg and Foxp3^{GPF} mice were labeled with 1 μM Cell Trace Violet (Life Technologies, OR, USA). Tregs were co-cultured with Cell Trace Violet labeled different effector cells (5×10^{4}) at indicated ratios in the presence of soluble anti-CD3 (1 μg/ml), anti-CD28 (1 μg/ml) and Mitomycin-treated splenic cells (1×10^{5}). After a 72 hour co-culture, cells were stained with Propidium Iodide Solution (Biolegend, San Diego, CA) for 10 min to exclude dead cells, and T cell proliferation assessed by Cell Trace Violet dilution. The proliferation index was defined as the ratio of final cell count to initial cell number as previously described [25].

Tissue Histology

Immediately after sacrifice, liver tissues were fixed with 10% buffered formalin at room temperature for 48 hours, then embedded in paraffin; liver tissues was cut into 4-μm sections. Liver sections were deparaffinized, stained with hematoxylin and eosin (H&E). Histological scores were evaluated by “blinded” pathologist (K.T.). Firstly, the degree of portal inflammation was evaluated and scored as previously described [26], briefly: 0, normal liver histology, no inflammatory cells; 1, minimal inflammation, several mononuclear cells; 2, mild inflammation, mild lympho-plasmycytic infiltration without interface hepatitis; 3, moderate inflammation, mild lympho-plasmacytic infiltration with interface hepatitis; and 4, severe inflammation, moderate-severe lympho-plasmacytic infiltration with interface hepatitis. In addition, the degree of overall liver inflammation was determined by the percentage of affected tissue within the total hepatic lobules per specimen and coded as follows: 0, none, 1, 1%–10%; 2, 11–20%; 3, 21–50%; 4, more than 50%. Finally, a summary score that includes severity and frequency analysis was generated as the sum of these scores. Second, bile duct damage was evaluated firstly by the degree of severity in the most severe lesions as follows: 0, no significant changes of bile duct; 0.5, ;1, epithelial damage (only cytoplasmic change); 2, epithelial damage with cytoplasmic and nuclear change; 3, non-suppurative destructive cholangitis (CNSDC); 4, bile duct loss. The frequency of bile duct damage was scored as follows: 0, none; 1, 1%–10%; 2, 11–20%; 3, 21–50%; 4, more than 50%. Finally, to integrate the evaluation, the scores of severity and frequency were added together.

Antimitochondrial Antibodies (AMAs)

Serum AMAs were detected by ELISA with the recombinant E2 component of pyruvate dehydrogenase (PDC-E2), 2-oxo-glutarate dehydrogenase (OGDC-E2) and branched chain 2-oxo-acid dehydrogenase (BCOADC-E2) [8]. AMAs were also detected by immunoblotting as described [27].

Statistical Analysis

Data are presented as the mean ± standard deviation (SD). The significance of differences was determined using a two-tailed unpaired t test or the Mann-Whitney U test in Graph Pad Prism; the significance levels are noted * $P < 0.05$; ** $P < 0.01$; *** $P < 0.001$.

Results

1. Absence of CD4$^+$ T cells leads to severe aggravated cholangitis

In the absence of CD4$^+$ T cells, CD4$^{-/-}$Tg mice exhibited more severe portal inflammation (P=0.0017) and bile duct damage (P=0.03) (Figure 1A, B). Flow cytometry demonstrated that although the total mononuclear cells number in CD4$^{-/-}$Tg in liver, spleen and mLN was statistically unchanged compared to Tg mice (Figure 2A), the total number of hepatic CD8$^+$ T cells (NK1.1$^-$CD3$^+$CD8$^+$) (P=0.045) and invariant natural killer T cells (P=0.005) were increased (Figure 2B). The number of IFN-γ$^+$ CD8$^+$ T cells increased significantly in CD4$^{-/-}$Tg mice (P=0.047) (Figure 2C, D), but the frequency of IFN-γ$^+$ cells in CD8$^+$ T cells did not differ (P=0.59) (Figure 2C, D). In the spleen, both the percentage and total IFN-γ$^+$ CD8$^+$ T cells increased (P=0.016) (Figure 2C, D). Overall, these data suggest that loss of CD4$^+$ T cells results in increased numbers of highly inflammatory CD8$^+$ T cells. To study the direct interaction between Tregs and effector cells, i.e. non-Treg CD4$^+$ T cells and CD8$^+$ T cells, Tregs from Foxp3^{GFP} and Foxp3^{GFP}Tg mice were co-cultured with effector responder cells *in vitro*. Tg mice derived Tregs suppressed both CD4$^+$ conventional T cells and CD8$^+$ T cells (Figure 3A), but reduced suppression compared to WT Tregs (Figure 3B). These data collectively suggest that the CD8 mediated pathology in CD4$^{-/-}$Tg mice are secondary to loss of the critical CD4 Treg subset.

2. Parabiosis of WT mice to CD4$^{-/-}$Tg mice successfully treats biliary disease

After parabiosis (Figure 4A) to WT mice, CD4$^{-/-}$Tg mice exhibited no biliary disease (Figure 4B). Serum AMA levels in each parabiont were similar to CD4$^{-/-}$Tg mice and control WT mice (Figure 4C,D). Hence, introducing normal CD4$^+$ T cells reversed a disordered immune system. Lymphocytes from liver after parabiosis were tested by flow cytometry. Quantification of CD45 subsets confirmed that more WT leukocytes were found in CD4$^{-/-}$Tg liver, than CD4$^{-/-}$Tg leukocytes in WT liver (Figure 5A). Further cell subset analysis revealed that CD4$^{-/-}$Tg -derived hepatic T lymphocytes and invariant NKT cells were dramatically decreased in the HMNC of CD4$^{-/-}$Tg mice, while CD4$^{-/-}$ derived T cells and iNKT cells demonstrated no decline in CD4$^{-/-}$ hosts (Figure 5B). Indeed, WT parabiont-derived CD4$^+$CD25$^+$Foxp3$^+$ Tregs were the main source of the entire Treg fraction in the parabiosised pair, and the Treg frequency in CD4$^+$ T cells remained normal (Figure 5C). Introducing wild type CD4$^+$ T cells, including Tregs, to CD4$^{-/-}$Tg mice, led to the deletion of over-reactive CD8$^+$ T cells, as well as the activation and capacity of cytokine secretion of the remaining CD8$^+$ T cells were decreased (Figure 5D,E). Moreover, CD4$^{-/-}$Tg mice derived B cells increased and became the most abundant lymphocyte subpopulations derived from CD4$^{-/-}$Tg mice.

3. Mice reconstituted with BM from both CD4$^{-/-}$Tg and CD8$^{-/-}$ mice are significantly protected from cholangitis

We should emphasize that to avoid the effect of WT CD8$^+$ T cells in chimeras, CD8$^{-/-}$ CD45.1 mice were used and lineage negative bone marrow mixed in equal proportion using bone marrow cells from CD4$^{-/-}$Tg CD45.2 mice. Single BMT control groups received CD4$^{-/-}$Tg CD45.2 bone marrow. Congenic CD45.1&CD45.2 mice served as recipients, as shown in Figure 6A. Recipients of CD4$^{-/-}$Tg alone developed more severe portal

inflammation (P=0.002) and a relatively higher incidence of bile duct damage (56%: 33%), compared with recipients of mixed bone marrow (Figure 6B,C). Further phenotypic and functional analysis of mixed bone marrow chimeric mice (Figure 7A) demonstrate that total hepatic mononuclear cells, (P=0.0203) (Figure 7B), T cell number (P=0.0096) and terminally differentiated $CD8^+$ effector memory T cells (P=0.030) from mixed BMC mice were all less than single BMC mice (Figure 7C). Natural killer cells (P=0.0087) and B cells (P=0.0045), derived from $CD4^{-/-}$Tg mice in mixed BMC mice were also less than single BMC mice (Figure 7C). Importantly, bone marrow-derived cells from $CD8^{-/-}$ CD45.1 mice induced normal frequency of $CD4^+Foxp3^+$ Tregs in $CD4^+$ T cells reconstitution, and Tregs also expressed conventional Tregs surface markers such as CD25, cytotoxic T lymphocytes-associated antigen (CTLA-4, CD152) and glucocorticoid-induced tumor necrosis factor receptor (GITR) (Figure 7D). These data suggest that normal $CD4^+$ T cells could rescue an ongoing autoimmune cholangitis.

Discussion

We report herein successful treatment of established autoimmune cholangitis, both by parabiosis and generation of chimeras. Indeed, it is the Treg fraction of the CD4 population that mediates these effects. This conclusion is supported not only by the *in vivo* histology, but also by the *in vitro* suppression assays. For example, we note that there is decreased suppressive activity of Tregs derived from Tg mice directed at both CD4 and CD8 conventional T cells, as compared with WT Tregs. These data are consistent with our recent analysis of Tregs at the level of both transcription and pathway analysis [28]. We should also note that although Tregs derived from Tg are compromised, they still retain some suppressive function.

We used parabiosis to generate circulating chimeras of $CD4^{-/-}$Tg mice and WT mice, so as to investigate whether introducing normal leukocytes from WT mice would reverse the established immune disorder in $CD4^{-/-}$Tg mice. Introducing normal CD4 T cells into $CD4^{-/-}$Tg mice may also give rise to the Tregs fraction in liver. After parabiosis, $CD4^{-/-}$Tg mice recovered from biliary disease. Our most important observation was the decrease of $CD4^{-/-}$Tg host derived activated $CD8^+$ T cells. This data reveals that wild type leucocytes reversed inflammation in $CD4^{-/-}$Tg mice. Another feature in our parabiosis model was the dramatic decrease of hepatic resident cells, i.e. iNKT and NK cells in liver. Further studies should focus on how the inflammation response changes the micro-environment of liver.

Next we determined whether adding back WT $CD4^+$ cells into $CD4^{-/-}$Tg mice was sufficient to reverse an established immune. In mixed chimeric mice, compared to single BMC $CD4^{-/-}$Tg recipients, there were fewer effector $CD8^+$ T cells, especially terminal differentiated $KLRG1^+$ $CD8^+$ T cells. This data is in accordance with our previous work, which showed mixed Tg and wild type bone marrow chimeric mice were protected from cholangitis compared to Tg single bone marrow chimeras [20]. The present work, however, focused on excluding the influence of Tg mice derived Tregs and non-Treg conventional $CD4^+$ T cells. Terminal differentiated $KLRG1^+$ $CD8^+$ T cells are enriched in antigen specific cells [29–31]. Limiting the $CD8^+$ T cell repertoire to ovalbumin (OVA) in Tg mice (OT I-Tg-$RAG1^{-/-}$) demonstrates the existence of auto antigen specific $CD8^+$ T cells in Tg mice

[15]. Thus, there is the attractive possibility that regulatory T cells from wild type mice alleviates biliary disease by limiting the differentiation of autoantigen specific $CD8^+$ T cells. Future studies should also focus on antigen specific $CD8^+$ T cell subpopulations and the likelihood that there truly exists regulatory specific T cells. We also suggest that cholangitis in this model involves a responder cell related suppressive pathway that is partially independent of TGFβ signaling. These data have implications for human patients with PBC. Firstly, although defects in T regulatory cells have been demonstrated in a variety of autoimmune diseases, there is a paucity of data on the specific pathways involved and the likelihood of antigen-specific defects. Second, the data suggests that in an antigen-specific autoimmune disease, improvement of Treg function would have clinical application even in hosts with established disease.

Conclusion

CD4 deficiency in Tg mice led to more severe biliary disease, and adding back wild type $CD4^+$ T cells, containing Tregs, by bone marrow transplantation or parabiosis extenuated the biliary disease. These results demonstrated that normal $CD4^+$ T cells from a healthy donor can act therapeutically on established PBC.

Acknowledgments

Financial support: Financial support provided by the National Basic Research Program of China (973 Program-2013CB944900), the National Natural Science Foundation of China (81130058, 81430034), the Research Fund for the Doctoral Program of Higher Education of China (RFDP 20133402110015), and NIH 2R01DK090019-05 (MEG).

Abbreviations

Tg	Dominant negative transforming growth factor β receptor II
PBC	primary biliary cirrhosis
Tregs	regulatory T cells
mLN	mesenteric lymph node
WT	wild type
MNC	mononuclear cells
IFN-γ	interferon-γ
BMT	bone marrow transplantation
BMC	bone marrow chimera
Tem	effector memory T cells
Tn	Naïve T cells
Tcm	central memory T cells.

References

1. Kaplan MM, Gershwin ME. Primary biliary cirrhosis. N Engl J Med. 2005; 353(12):1261–73. [PubMed: 16177252]
2. Hirschfield GM, Gershwin ME. The immunobiology and pathophysiology of primary biliary cirrhosis. Annu Rev Pathol. 2013; 8:303–30. [PubMed: 23347352]
3. Li Y, et al. Chemokine (C-X-C motif) ligand 13 promotes intrahepatic chemokine (C-X-C motif) receptor 5+ lymphocyte homing and aberrant B-cell immune responses in primary biliary cirrhosis. Hepatology. 2015; 61(6):1998–2007. [PubMed: 25627620]
4. Wang L, et al. Breach of tolerance: primary biliary cirrhosis. Semin Liver Dis. 2014; 34(3):297–317. [PubMed: 25057953]
5. Zhang J, et al. Ongoing activation of autoantigen-specific B cells in primary biliary cirrhosis. Hepatology. 2014; 60(5):1708–16. [PubMed: 25043065]
6. Wang L, et al. CXCR5+ CD4+ T follicular helper cells participate in the pathogenesis of primary biliary cirrhosis. Hepatology. 2015; 61(2):627–38. [PubMed: 25042122]
7. Lleo A, et al. Shotgun proteomics: identification of unique protein profiles of apoptotic bodies from biliary epithelial cells. Hepatology. 2014; 60(4):1314–23. [PubMed: 24841946]
8. Oertelt S, et al. Anti-mitochondrial antibodies and primary biliary cirrhosis in TGF-beta receptor II dominant-negative mice. J Immunol. 2006; 177(3):1655–60. [PubMed: 16849474]
9. Yang GX, et al. Adoptive transfer of CD8(+) T cells from transforming growth factor beta receptor type II (dominant negative form) induces autoimmune cholangitis in mice. Hepatology. 2008; 47(6): 1974–1982. [PubMed: 18452147]
10. Moritoki Y, et al. B-cell depletion with anti-CD20 ameliorates autoimmune cholangitis but exacerbates colitis in transforming growth factor-beta receptor II dominant negative mice. Hepatology. 2009; 50(6):1893–903. [PubMed: 19877182]
11. Moritoki Y, et al. B Cells Suppress the Inflammatory Response in a Mouse Model of Primary Biliary Cirrhosis. Gastroenterology. 2009; 136(3):1037–1047. [PubMed: 19118554]
12. Zhang W, et al. Deletion of interleukin-6 in mice with the dominant negative form of transforming growth factor beta receptor II improves colitis but exacerbates autoimmune cholangitis. Hepatology. 2010; 52(1):215–22. [PubMed: 20578264]
13. Ando Y, et al. The immunobiology of colitis and cholangitis in interleukin-23p19 and interleukin-17A deleted dominant negative form of transforming growth factor beta receptor type II mice. Hepatology. 2012; 56(4):1418–26. [PubMed: 22532156]
14. Tsuda M, et al. Deletion of interleukin (IL)-12p35 induces liver fibrosis in dominant-negative TGFbeta receptor type II mice. Hepatology. 2013; 57(2):806–16. [PubMed: 22576253]
15. Kawata K, et al. Clonality, activated antigen-specific CD8(+) T cells, and development of autoimmune cholangitis in dnTGFbetaRII mice. Hepatology. 2013; 58(3):1094–104. [PubMed: 23532950]
16. Sakaguchi S, et al. Regulatory T cells and immune tolerance. Cell. 2008; 133(5):775–87. [PubMed: 18510923]
17. Lan RY, et al. Liver-targeted and peripheral blood alterations of regulatory T cells in primary biliary cirrhosis. Hepatology. 2006; 43(4):729–737. [PubMed: 16557534]
18. Aoki CA, et al. IL-2 receptor alpha deficiency and features of primary biliary cirrhosis. J Autoimmun. 2006; 27(1):50–3. [PubMed: 16904870]
19. Wakabayashi K, et al. IL-2 receptor alpha(−/−) mice and the development of primary biliary cirrhosis. Hepatology. 2006; 44(5):1240–9. [PubMed: 17058261]
20. Huang W, et al. Murine autoimmune cholangitis requires two hits: cytotoxic KLRG1(+) CD8 effector cells and defective T regulatory cells. J Autoimmun. 2014; 50:123–34. [PubMed: 24556277]
21. Tanaka H, et al. Successful Immunotherapy of Autoimmune Cholangitis by Adoptive Transfer of Foxp3 Regulatory T cells. Clin Exp Immunol. 2014

22. Donskoy E, Goldschneider I. Thymocytopoiesis is maintained by blood-borne precursors throughout postnatal life. A study in parabiotic mice. J Immunol. 1992; 148(6):1604–12. [PubMed: 1347301]
23. Kamran P, et al. Parabiosis in mice: a detailed protocol. J Vis Exp. 2013; (80)
24. Kruisbeek AM, Shevach E, Thornton AM. Proliferative assays for T cell function. Curr Protoc Immunol. 2004 Chapter 3: p. Unit 3 12.
25. Hawkins ED, et al. Measuring lymphocyte proliferation, survival and differentiation using CFSE time-series data. Nat Protoc. 2007; 2(9):2057–67. [PubMed: 17853861]
26. Yang W, et al. Differential modulation by IL-17A of Cholangitis versus Colitis in IL-2Ralpha deleted mice. PLoS One. 2014; 9(8):e105351. [PubMed: 25133396]
27. Moteki S, et al. Use of a designer triple expression hybrid clone for three different lipoyl domain for the detection of antimitochondrial autoantibodies. Hepatology. 1996; 24(1):97–103. [PubMed: 8707289]
28. Wang YH, et al. Systems biologic analysis of T regulatory cells genetic pathways in murine primary biliary cirrhosis. J Autoimmun. 2015
29. Bengsch B, et al. Analysis of CD127 and KLRG1 expression on hepatitis C virus-specific CD8+ T cells reveals the existence of different memory T-cell subsets in the peripheral blood and liver. J Virol. 2007; 81(2):945–53. [PubMed: 17079288]
30. Cush SS, Flano E. KLRG1+NKG2A+ CD8 T cells mediate protection and participate in memory responses during gamma-herpesvirus infection. J Immunol. 2011; 186(7):4051–8. [PubMed: 21346231]
31. Thimme R, et al. Increased expression of the NK cell receptor KLRG1 by virus-specific CD8 T cells during persistent antigen stimulation. J Virol. 2005; 79(18):12112–6. [PubMed: 16140789]

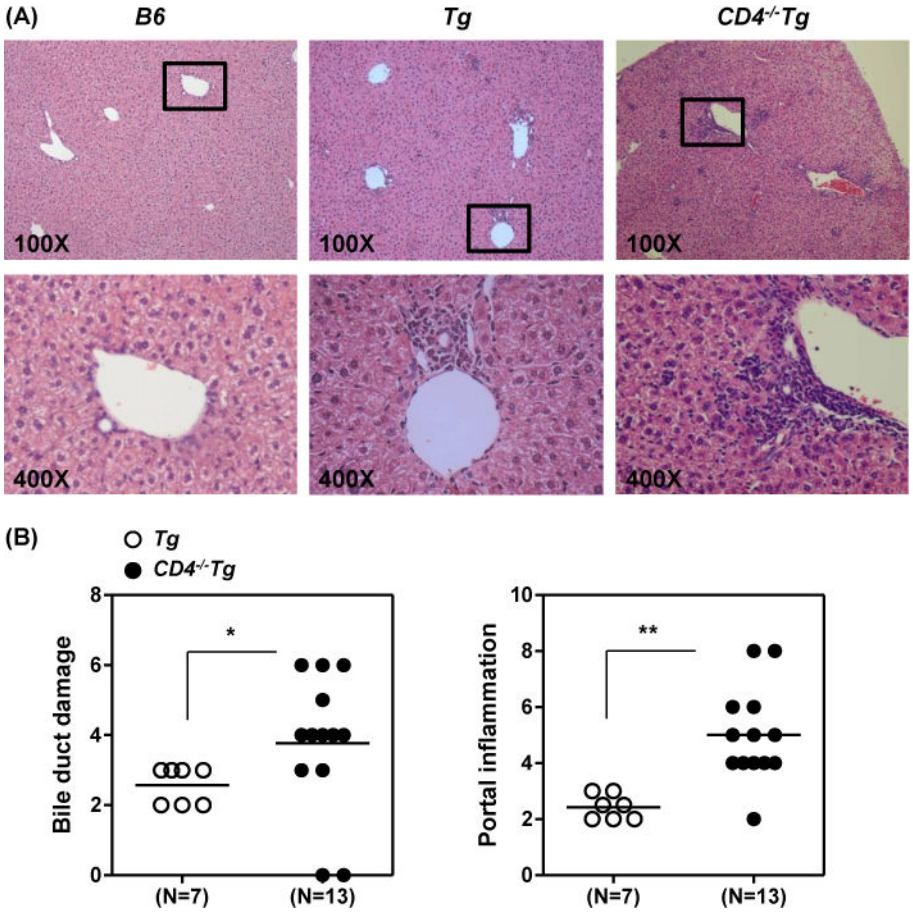

Figure 1. CD4 deficient Tg mice developed more severe cholangitis

(A) HE-stained liver sections of wild type B6, Tg and CD4$^{-/-}$Tg mice at 14 to 16 weeks of age demonstrated portal tract inflammation and bile duct damage. (B) Scores of bile duct damage and portal inflammation in Tg mice (blank circle, N=7) and CD4$^{-/-}$Tg mice (filled circle, N=11). Each symbol represents one mouse; small horizontal lines indicate the mean. *P <0.05, **P <0.01 as determined by the Mann-Whitney U test.

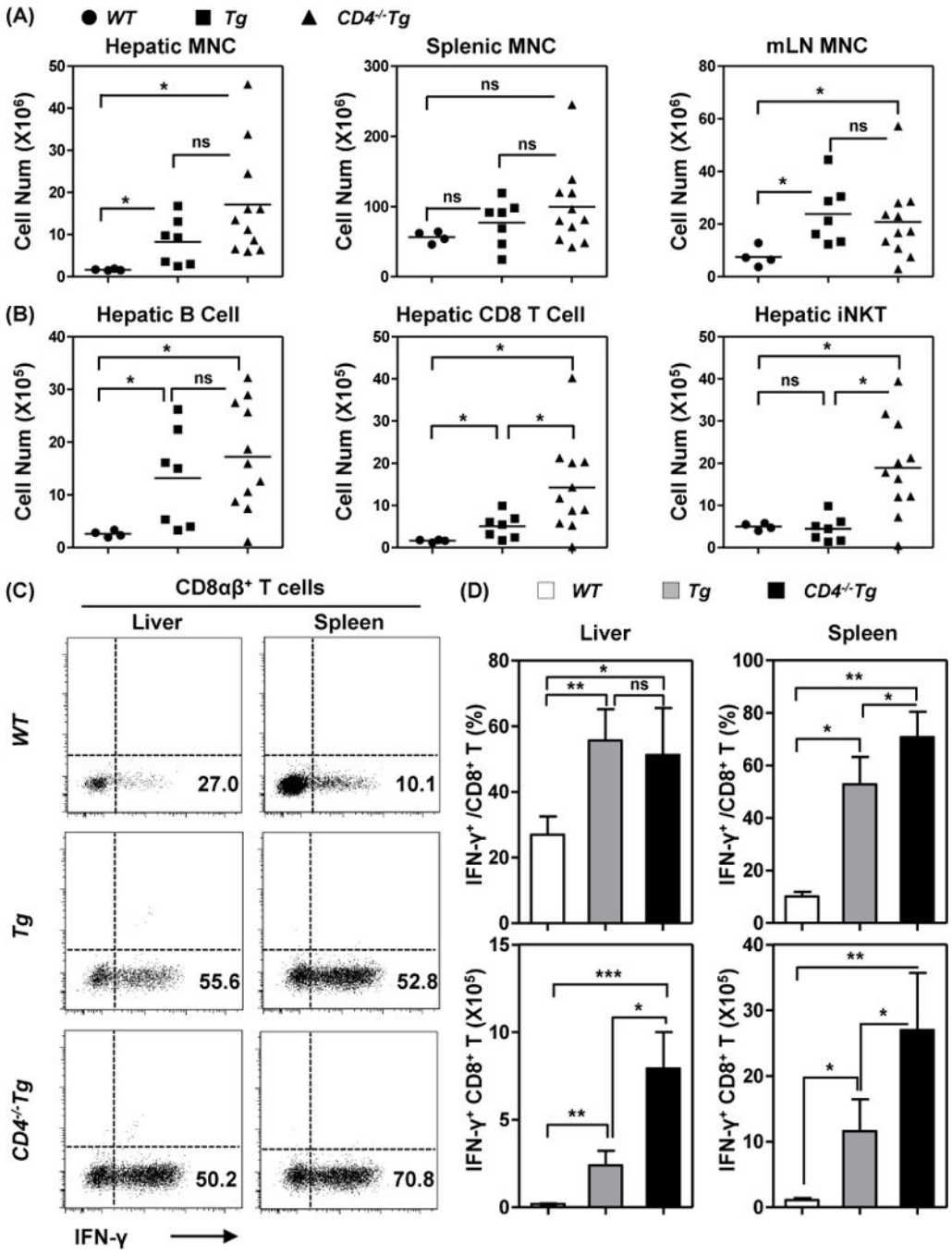

Figure 2. CD4 deficient Tg mice develop more pathogenic CD8 T cells than Tg mice

(A) The absolute number of mononuclear cells of liver, spleen and mesenteric lymph nodes from wild type (N=4), Tg (N=7) and $CD4^{-/-}$Tg mice (N=11). (B) The absolute number of B cells ($CD19^{+}$), CD8 T cells ($NK1.1^{-}CD3^{+}CD8^{+}$) and invariant natural killer T cells (α-Galcer-CD1d-$Tetramer^{+}CD3^{+}$) in liver from Tg (N=7) and $CD4^{-/-}$Tg mice (N=11). Each symbol represents one mouse; small horizontal lines indicate the mean. (C) Mononuclear cells from liver and spleen were stimulated with PMA and ionomycin for 3 hours in the presence of Golgi stop reagent. Secreted IFN-γ was assessed by flow cytometric analysis.

(D) Frequency of IFN-γ^+ cells in CD8 T cells (upper panel) and total IFN-γ^+ CD8 T cells numbers (lower panel) in liver and spleen from wild type (N=4), Tg (N=7) and $CD4^{-/-}$Tg mice (N=11). Data are representative of two independent experiments with similar results. *P <0.05, **P <0.01 and ***P <0.001 as determined by Student Test.

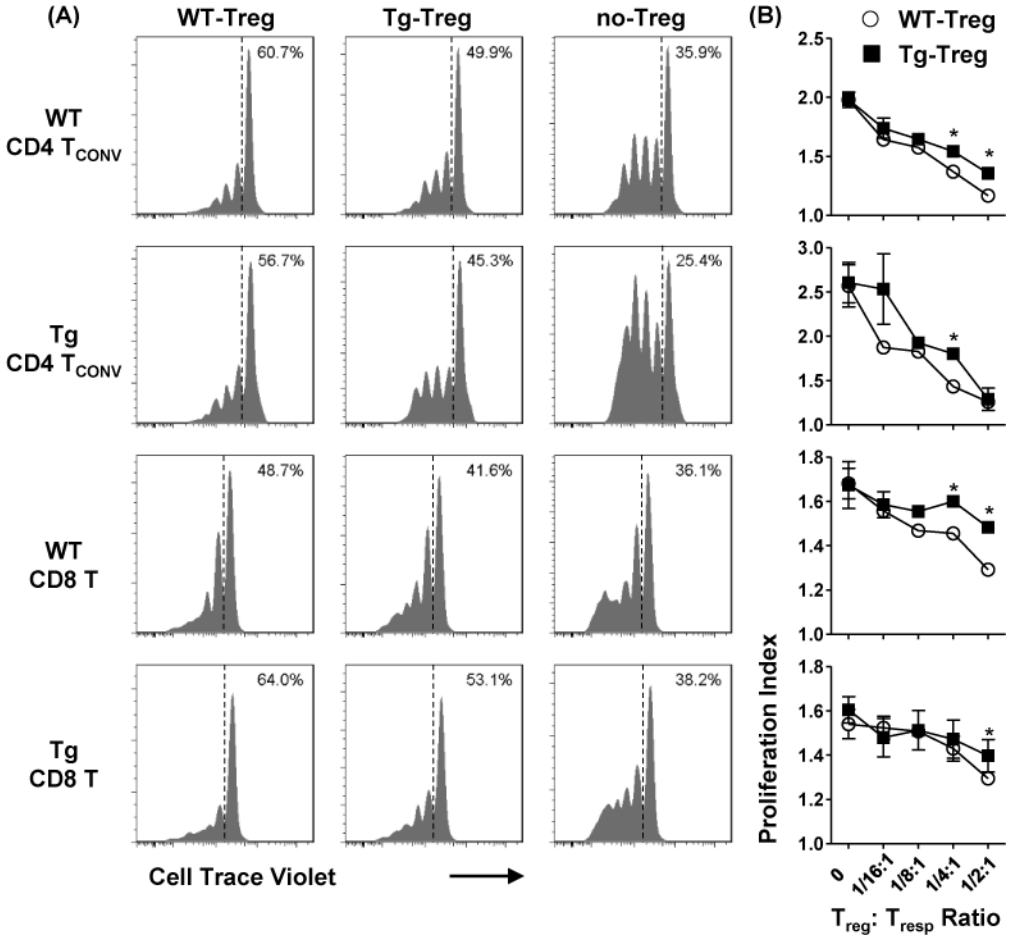

Figure 3. Tg-derived Tregs have impaired suppressive function in vitro

In vitro proliferation of responder T cells ($CD4^+$ $Foxp3^-$ conventional cells, non-Tregs $CD4^+$ T, and $CD8^+$ T cells from the spleen of WT and Tg mice, respectively) co-cultured at various ratios (horizontal axis in (B)) for 72 hour with Tregs sorted from splenocytes of $Foxp3^{GFP}$ and $Foxp3^{GFP}$Tg mice, assessed as the dilution of Cell Trace Violet. (A) Representative flow cytometry profiles are shown, the ratio of Tregs to responder cells is 1 to 4. (B) Reprehensive the proliferation index at graded cultured ratio, white circles represented WT-Treg co-cultured with responder cells, black square represented Tg-Treg co-cultured with responder cells. Data are representative of two experiments. *P <0.05 as determined by Student Test.

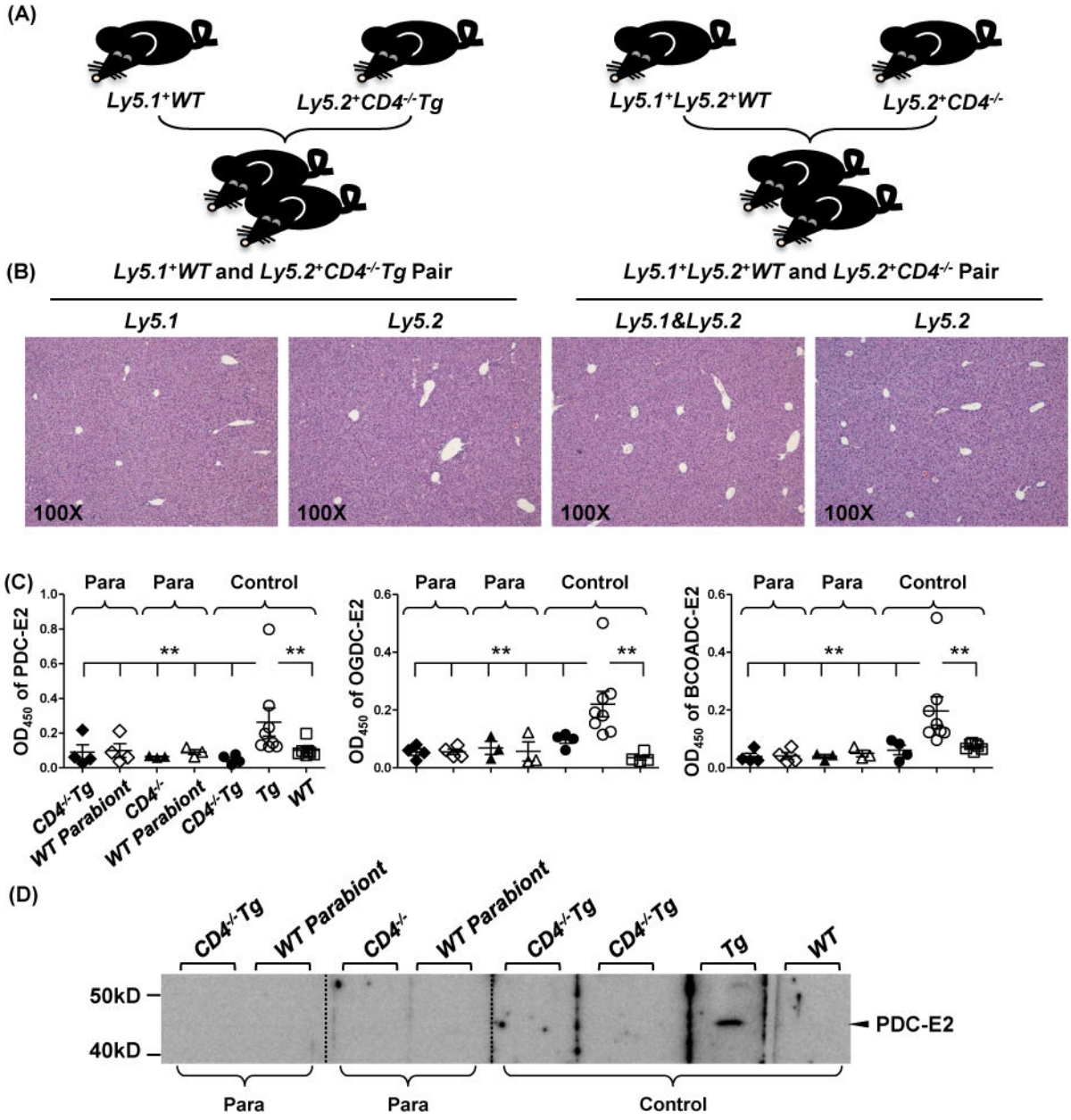

Figure 4. Parabiosis of CD4$^{-/-}$Tg mice to WT mice attenuates biliary disease

(A) Parabiosis strategy: Ly5.2^{+}CD4$^{-/-}$Tg mice were parabiosised to congenic Ly5.1^{+}WT mice (N=4). Ly5.2^{+}CD4$^{-/-}$ mice parabiosised with congenic Ly5.1&Ly5.2^{+}WT mice served as controls (N=4). 4 weeks after surgery, the livers and spleens of parabiotic mice were harvested for both histopathology and flow cytometry. (B) Representative H&E analysis of liver tissue sections from Ly5.1^{+}WT mouse and Ly5.2^{+}CD4$^{-/-}$Tg mouse parabiotic pair (left two panels), Ly5.2^{+}CD4$^{-/-}$ mice and Ly5.1&Ly5.2^{+}WT parabiotic pair (right two panels). (C) Serum anti-PDC-E2 (left panel), anti-OGDC-E2 (middle panel), anti-BCOADC-E2 (right panel) antibodies from parabionts of CD4$^{-/-}$Tg (black filled diamond) with WT mice (empty diamond), CD4$^{-/-}$ (black filled triangle) with WT mice (empty triangle) were detected by ELISA. Non-parabiotic free 16 week-old CD4$^{-/-}$Tg (black circular), Tg (empty

circle) and WT mice (empty quadrate) served as controls. Serum samples were diluted 1:20. Horizontal bars represent median value. **P <0.01 as determined by the Mann-Whitney U test. (D) Levels of anti-PDC-E2 antibodies in serum from parabionts of $CD4^{-/-}$Tg and WT mice, $CD4^{-/-}$ and WT mice were tested by immunobloting after four weeks of parabiosis; along with non-parabiotic free age-matched $CD4^{-/-}$Tg (with repeats), Tg and WT mice served as controls. Serum samples were diluted 1:100.

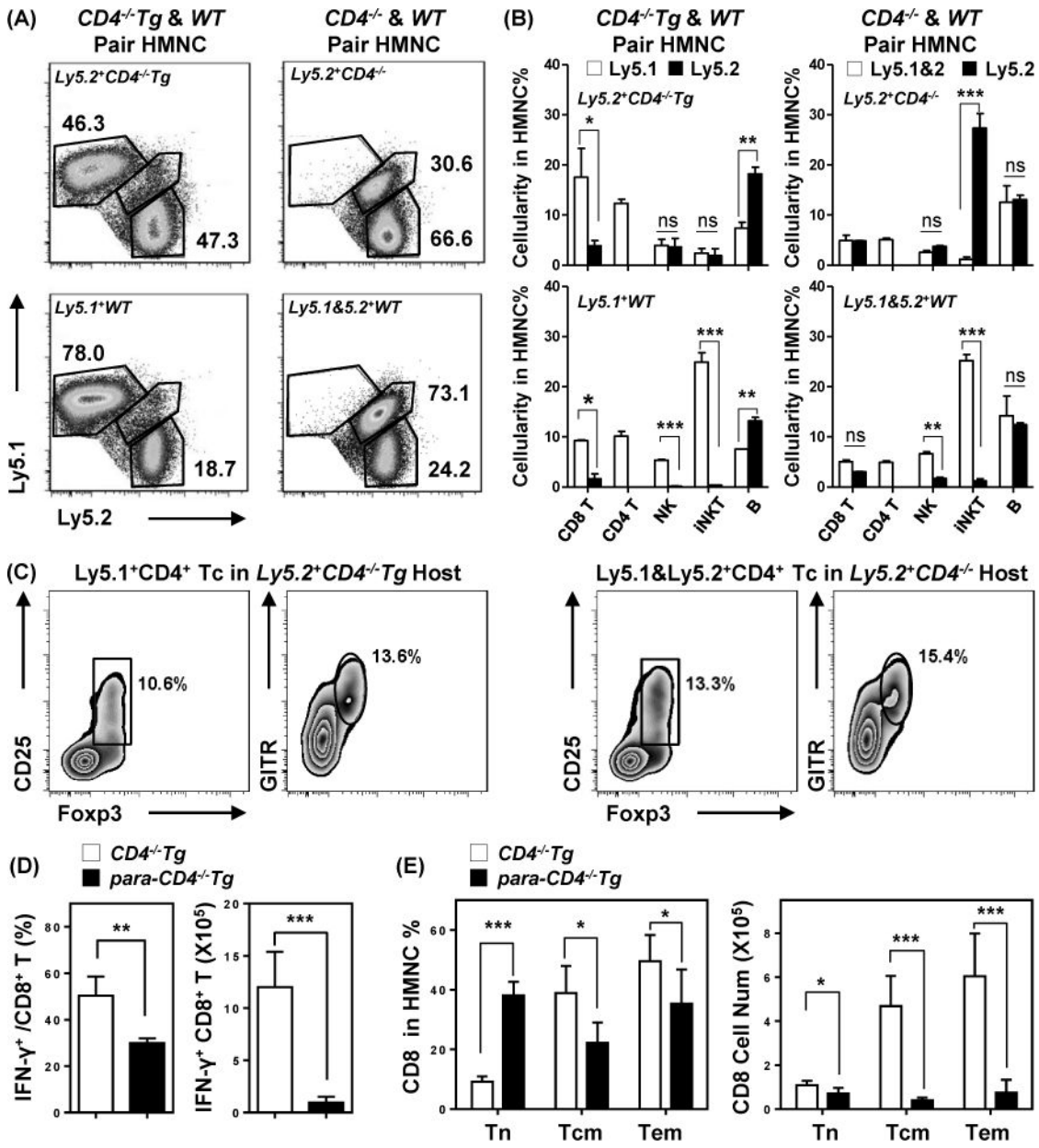

Figure 5. CD4$^{-/-}$Tg derived CD8^{+} T cells dramatic reduced after parabiosis to WT mice

(A) Representative dot plot of gated on hepatic mononuclear cells in liver (Ly5.1^{+}, Ly5.2^{+} or Ly5.1&Ly5.2^{+}) from 4 pairs of parabiotic mice. (B) Hepatic lymphocyte subpopulation distribution were determined by flow cytometry. The frequency of CD8^{+} T cells (CD3^{+} NK1.1^{-} CD8α^{+}), CD4 T cells (CD3^{+} NK1.1^{-} CD4^{+}), NK (CD3^{-} CD1d-tetramer^{-} NK1.1^{+}), invariant NKT cells (CD3^{+} CD1d-Tetramer^{+} NK1.1^{+}), B cells (CD3^{-} NK1.1^{-} CD19^{+}) in total hepatic mononuclear cells from different parabionts. (C) Representative flow cytometry profile of CD25^{+}Foxp3^{+} or GITR^{+}Foxp3^{+} Treg in CD4^{+} T cells in Ly5.1^{+}WT mice or Ly5.1&Ly5.2^{+}WT mice parabionts. (D) Frequency and the total number of IFN-γ+ cells in CD8 T cells in liver from CD4−/−Tg mice (N=7) and parabiotic CD4−/−Tg mice (N=4). (E) Frequency and the total number of CD8 T cells subsets in liver from from CD4−/−Tg mice

(N=7) and parabiotic CD4−/−Tg mice (N=4). *P <0.05, **P <0.01 and ***P <0.001 as determined by Student Test.

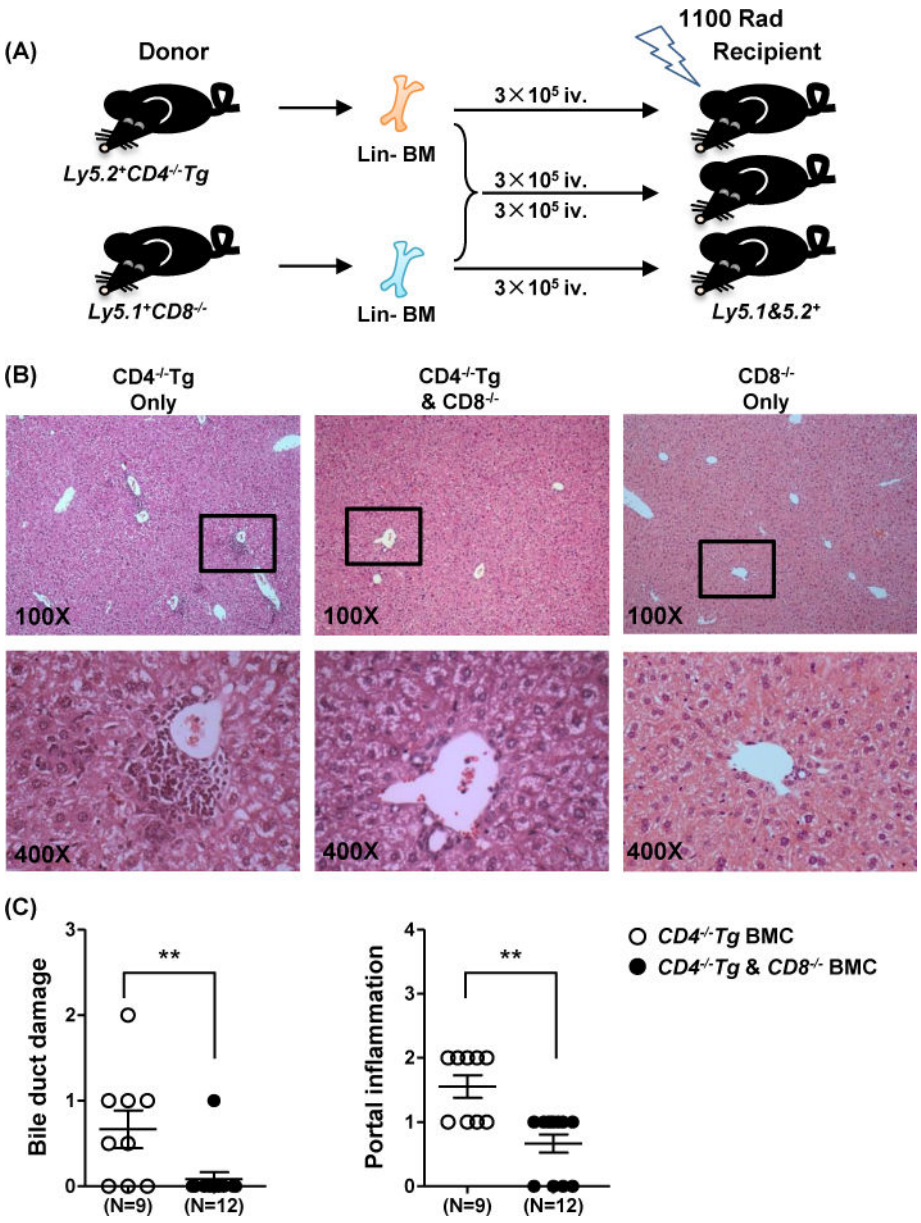

Figure 6. Mixed BMT mice had reduced autoimmune biliary disease compared with single CD4$^{-/-}$Tg BMT mice

(A) Bone marrow transplantation strategy: 3×10^5 lineage negative donor derived bone marrow cells were transplanted into 1100 rad γ-ray irradiated congenic mice. Two months later, mice were sacrificed. (B) Representative H&E analysis of liver tissue sections from CD4$^{-/-}$Tg single BMT chimeric mice, CD8$^{-/-}$ and CD4$^{-/-}$Tg mixed BMT chimeric mice and CD8$^{-/-}$ single BMT chimeric mice. (D) Scores of bile duct damage and portal inflammation in CD4$^{-/-}$Tg single BMT chimeric mice (blank circle, N=9), CD4$^{-/-}$Tg mixed BMT chimeric mice (filled circle, N=12). CD8$^{-/-}$ single BMT chimeric mice were also tested, and had no pathology. Each symbol represents one mouse; small horizontal lines indicate the mean. Only the degree of bile duct damage and portal inflammation were evaluated and scored. *P <0.05, **P <0.01 as determined by the Mann-Whitney U test.

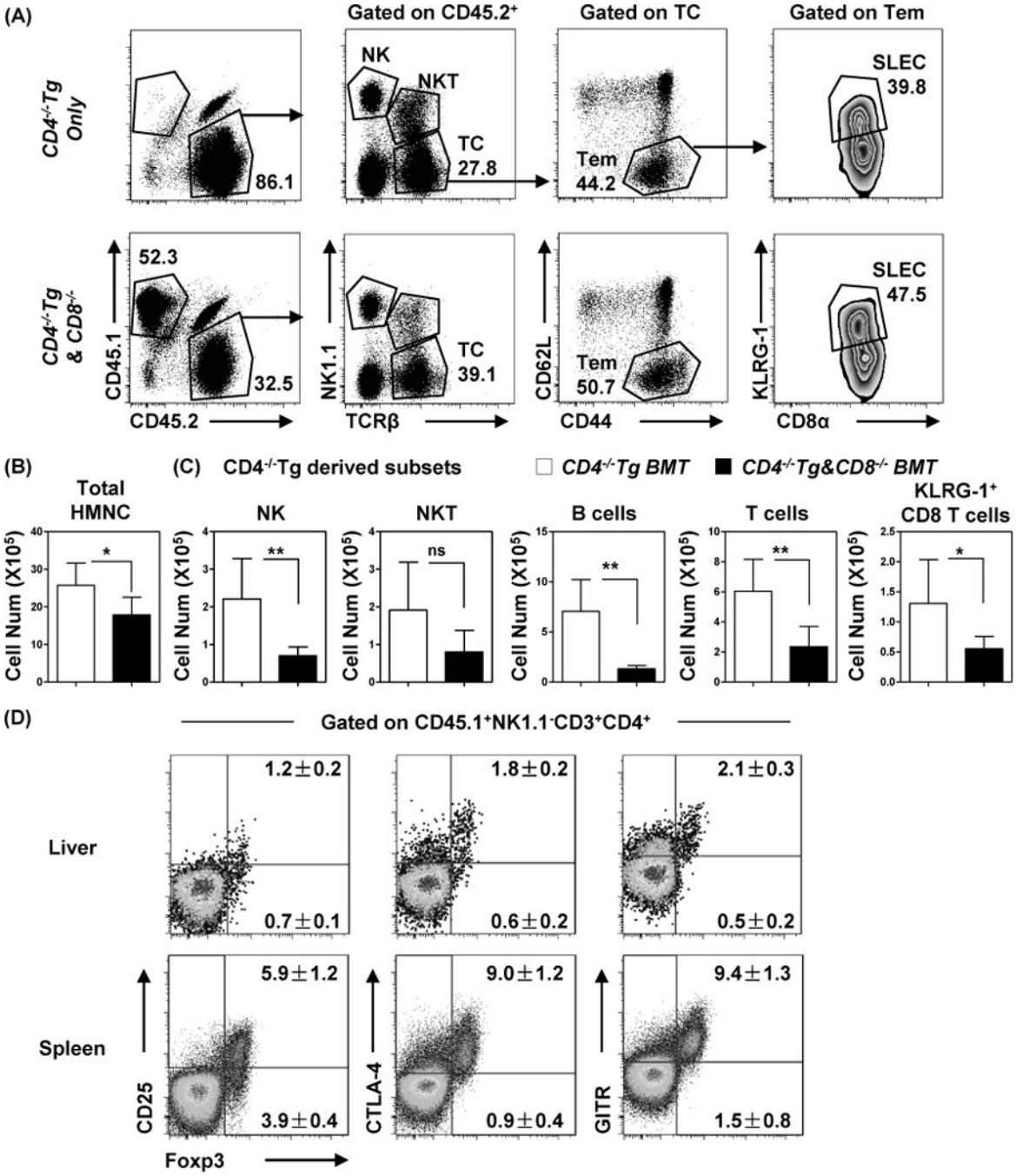

Figure 7. Hepatic mononuclear cell subsets of mixed BMT mice and CD4$^{-/-}$Tg mice single BMT mice

(A) Gating strategy used in FACS analysis. Left panel indicates the average frequency from two donors. NK (TCR-β^{-}NK1.1^{+}) reflect natural killer cells, NKT (TCR-β^{+}NK1.1^{+}) reflect natural killer T cells, TC (TCR-β^{+}NK1.1^{-}) reflect T cells. CD44^{+}CD62L^{-} T cells were defined as effector memory T cells (Tem). KLRG-1^{+} Tem cells were defined as short lived effector CD8^{+} T cells (SLEC). (B) Total hepatic lymphocytes number in recipient mice that received mixed bone marrow and single CD4$^{-/-}$Tg mice derived bone marrow. (C) Representative total cell number of CD4$^{-/-}$Tg mice derived NK cells, NKT cells, B cells, T

cells, effector memory CD8 T cell, Short lived effector T cells (KLRG-1^+ CD8 Tem cells) in mixed BMT mice and single BMT mice were assessed by FACS. (D) Flow cytometry profiles of CD25, CTLA4, GITR on $CD4^+Foxp3^+$ Tregs from $Ly5.1^+CD8^{-/-}$ mice in the livers and spleens of mixed bone marrow chimeric mice. Numbers in graphs present mean ± SD. *P <0.05, **P <0.01 as determined by Student Test.